SHADED-RELIEFS MATCHING AS AN EFFICIENT TECHNIQUE FOR 3D GEO-REFERENCING OF HISTORICAL DIGITAL ELEVATION MODELS

F.J. Aguilar [a, *], I. Fernández [a], M.A. Aguilar [a], J.L. Pérez [b], J. Delgado [b], J.G. Negreiros [c]

[a] Dept. of Agricultural Engineering, Almería University, La Cañada de San Urbano s/n, 04120 Almería, Spain - (faguilar, ismaelf, maguilar)@ual.es
[b] Dept. of Cartographic Engineering, Geodesy and Photogrammetry, Jaén University, Las Lagunillas s/n, 23071 Jaén, Spain – (jlperez, jdelgado)@ujaen.es
[c] ISEGI – University Nova de Lisboa, Campus de Campolide, Lisbon, Portugal - c8057@isegi.unl.pt

Commission VIII, WG9

KEY WORDS: Matching, DEM/DTM, Georeferencing, Coast, Shoreline, Monitoring

ABSTRACT:

Traditional methods using aerial photographs for shoreline measurement often involved non-stereo photography with no vertical information. However, digital elevation models (coastal elevation models or CEMs in our case) are widely used in GIS to predict the impact of coastal flooding and Sea Level Rise. Hence, we propose the CEM methodology to cope with computing shoreline position as the interface between the land and the water at a previously chosen vertical datum. Furthermore, CEM evolution during the studied period may be used to quantify the coastal landscape changes. In any case an accurate CEM is needed, both for newly-made CEMs and for historical CEMs mostly compiled from historical photogrammetric flights. A new approach to historical CEM 3D geo-referencing is proposed along this work to avoid the costly and time-consuming necessity of ground control points. The proposed methodology was tested for geo-referencing a historical grid format CEM, comprising a little coastal area of Almeria (South Spain), obtained by digital stereo-photogrammetry from a B&W photogrammetric flight taken in 1977 at an approximated scale of 1:18000. The reference CEM was the 10 m grid-spacing digital elevation model produced by the Andalusia Regional Government (Spain) coming from a 1:20000 scale W&B photogrammetric flight made in 2001. The results obtained from this work may be deemed as very promising, showing a high efficiency for historical CEM 3D geo-referencing when it was compared to traditional methods such as photogrammetric absolute orientation based on surveyed ground control points and self-calibrating bundle adjustment techniques. This preliminary approach could be used as a previous course matching to be subsequently refined by 3D robust surface matching.

1. INTRODUCTION

The coastal area is one of the greatest environmental and economic assets for a nation. Nowadays coastal vulnerability studies are experimenting a growing demand because the threatening tourism and construction development joined to the future scenario of widely predicted sea-level rise (SLR) and coastal flooding due to climate change (Titus et al., 2009). In fact, digital elevation models (coastal elevation models or CEMs in our particular case) are usually used to model SLR vulnerability (Cowell & Zeng, 2003) and coastal flood risk (Webster et al., 2006). Nowadays CEM production is efficiently accomplished by means of LiDAR technology which is contributing, often coupled with passive optical imaging, to a wide range of coastal scientific investigations (Brock & Purkis, 2009). However, as LiDAR is a relatively new technology, historical data beyond the past decade are practically unavailable (James et al., 2006). Let us remember that LiDAR mapping systems were not become available commercially till the late 90s. This is the reason because most of the studies headed up to obtain shoreline position and evolution along a certain period of time are mainly based on rectified aerial photographs, traditional and costly beach profiles from surveying techniques, topographic maps and so on. That is to say, traditional methods using aerial photographs for shoreline measurement often involved non-stereo photography with no vertical information. However, CEMs are widely used in GIS to predict the impact of coastal flooding and SLR. And more important, the accuracy of those CEMs is clearly bound to the reliability of the derived results (Aguilar et al., 2010a), as it is the case for maps of potential inundation along coastlines.

Hence, we propose the CEM-based methodology to cope with the following complementary objectives:

(i) to accurately compute shoreline position as the interface between the land and the water at a previously chosen vertical datum.
(ii) to use CEM evolution during the studied period to quantify the coastal landscape changes.

In any case an accurate CEM is necessary, both for newly-made CEMs obtained from, for instance, modern LiDAR technologies, and for historic CEMs mostly compiled from historic stereo photogrammetric flights. The latter approach requires a number of ground control points (GCPs) to compute the absolute orientation of every stereo pair, a surveying task that usually becomes inefficient and costly because the difficulty to accurately identify and survey a suitable set of ground points which could be pointed on the corresponding

---

* Corresponding author. This is useful to know for communication with the appropriate person in cases with more than one author.

historic photographs. Furthermore, in order to extract high quality topographic data from historical imagery, GCPs must also be of high quality and must be well distributed in the photographs (Aguilar et al., 2010b). This is especially important if camera calibration information is incomplete or unavailable (James et al., 2006). To avoid the necessity of ground control points, a new approach to historic CEM 3D geo-referencing is proposed along this work.

2. NEW APPROACH FUNDAMENTALS

The basic framework regarding the new approach fundamentals is shown in Fig. 1. Shortly, the proposed method starts from a course relative orientation of the historic CEM, compiled by stereo-photogrammetric techniques, where the stereo model y-parallax is removed by means of an Automatic Relative Orientation (ARO). Previously, the historical aerial photographs have to be scanned using a photogrammetric scanner. Subsequently, suitable photogrammetric software must be utilised, in this case ImageStation Digital Mensuration software (ISDM 4.0® from Z/I Imaging), to carry out ARO process. As it is widely known, ARO is the process that determines the relationship between two overlapping images, providing the position and attitude of one image with respect to another image by automatically matching tie points. Furthermore, it is highly recommendable to manually mark three control points (two full points XYZ and one only Z point) to apply a course seven parameters Helmert 3D transformation, obtaining a pre-oriented stereo-pair which will be very helpful to improve and speed up the convergence of the subsequent shaded-relief matching process. Those control points only have to present approximated coordinates, both horizontal and vertical, so they can be easily extracted from reference orthophotos (horizontal) and supposing a common Z (e.g. average ground height along the working area). In this way, a Digital Surface Model (DSM) or, after applying a filtering process, a DTM (Digital Terrain Model), both called generically CEMs from here onwards, can be obtained by means of stereo matching techniques ranking over digital images (Aguilar et al., 2007). ImageStation Automatic Elevations (ISAE 4.0® from Z/I Imaging) was the software used to generate DTM or DSM points from stereo-imagery, providing a large number of points by digital matching identical features in each of the stereo overviews.

Next a 2D shaded-relief is generated for both the historic CEM (model to geo-reference) and the reference CEM (a more recently obtained and already geo-referenced CEM). In this regards, different shaded-reliefs may be tested, only changing the solar elevation and azimuth, to optimize the final 3D matching between the historic and reference CEM. In this sense, the algorithm can be repeated till obtaining the best solution (Fig. 1).

An automatic matching algorithm based on the Scale Invariant Feature Transform (SIFT) has been implemented to identify conjugated points in image space (pixel coordinates) belonging to reference and historic CEM shaded-relief images. This algorithm is able to extract features invariant to image scale and rotation. Furthermore these features are shown to provide robust matching across a substantial range of affine distortion, change in 3D viewpoint, addition of noise, and change in illumination, so it can be deemed as very suitable to our practical application. The reader may find an in-depth description of SIFT method in Lowe (2004). This automatic approach turned out successful when the CEMs to match were relatively similar, but it did not when there was a great level of disparity between CEMs due to

important landscape modifications (mainly anthropogenic alterations brought about coastal area development). In this case a manual approach would be needed allowing a sub-pixel pointing on shaded-relief images (non presented data).

Finally, the 3D coordinates for every pair of conjugate points were automatically extracted from shaded-relief (UTM ETRS89 East and North) and CEMs (heights above GRS80 ellipsoid). Those pairs of 3D points, previously transformed to geocentric coordinates, allowed computing an iterative least squares registration between both CEMs by means of a robust seven parameters 3D Helmert transformation (Equation 1, where the orthonormal rotation matrix is represented by 3x3 elements which are trigonometric functions of the rotation angles Ω, Φ and K). The outliers found after each iteration were discarded and not taken into account in the next one by establishing a threshold value to avoid gross errors due to landscape changes (e.g. cut and fill earthworks, new buildings, etc.). That threshold was initially set up to the approximated uncertainty of the reference CEM, but sometimes had to be increased because at least three points were needed to compute the 3D Transformation.

$$\begin{bmatrix} X \\ Y \\ Z \end{bmatrix} = \lambda \begin{bmatrix} a_{11} & a_{12} & a_{13} \\ a_{21} & a_{22} & a_{23} \\ a_{31} & a_{32} & a_{33} \end{bmatrix} \begin{bmatrix} x \\ y \\ z \end{bmatrix} + \begin{bmatrix} \Delta X \\ \Delta Y \\ \Delta Z \end{bmatrix} \qquad (1)$$

Afterwards estimating the seven transformation parameters, 3D transformation was applied to historical CEM (using geocentric coordinates) to orientate it. All the processes constituting this basis framework, except for ARO and CEM generation, were programmed using MATLAB R2009®.
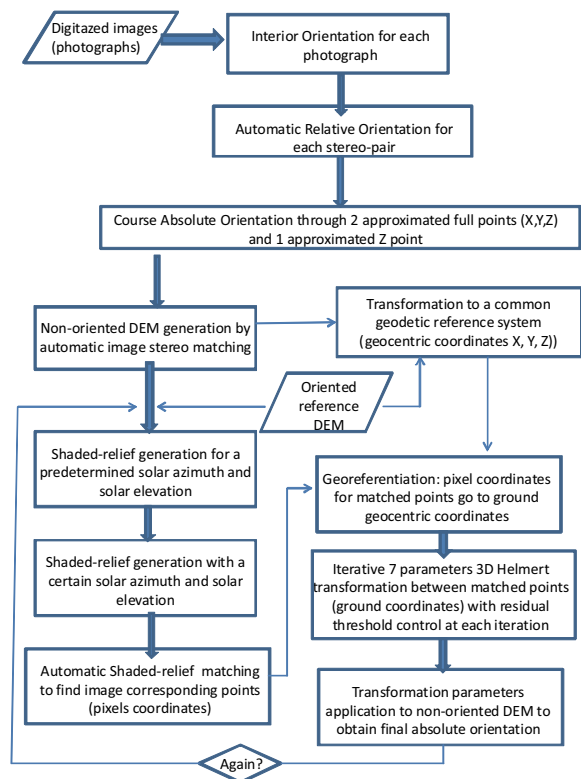

Figure 1. Flowchart diagram showing the algorithm framework.

3. STUDY SITE AND DATASETS

3.1 Study Site

The previously described shaded-relief image matching method was tested on one stereo-pair belonging to a historical photogrammetric flight which will be later described. The study area comprises a heavily developed coastal area of Almería (Mediterranean Sea, South Spain). The working area was concretely situated between the harbour of Garrucha and Antas dry-ravine mouth (Fig. 2). This is currently a high risk inundation zone joined to an urban area of high cultural density.

Figure 2. Coastal image showing the study site.

3.2 Datasets

3.2.1. Data corresponding to 1977: Come from an analogic W&B stereo-pair belonging to the so-called Agriculture photogrammetric flight. This flight presented an approximated scale of 1:18000 and focal distance around 152.77 mm. It was taken in 1977. A 10 m grid-spacing DSM was carried out by means of stereo matching techniques (ISAE 4.0® from Z/I Imaging) ranking over previously digitized images (15 microns per pixel ≈ 30 cm ground sample distance) with a spectral resolution of 8 bits. ISDM 4.0®, from Z/I Imaging, was used to carry out the preliminary coarse orientation by means of automatic relative orientation (see section 2).

Just for comparison purposes, a classical photogrammetric project was carried out to obtain the best possible absolute orientation of the 1977 tested stereo-pair. For it, Leica Photogrammetry Suite 9.1® (LPS) was utilised. Because our historical flight lacks of camera calibration certificate, which is very usual by the way, the corner coordinates for each photograph (fiducial marks) were established using precise manual measurements made on the positives. The principal point coordinates were fixed at zero, i.e. no offset existed between the principal point and the fiducial centre. Focal length was included because it usually appears as marginal data in aerial photographs. LPS allows applying different Additional Parameters (APs) models in the aerial triangulation process. The APs are the terms of a polynomial expression incorporated to the collinearity equations which allow the modelling of systematic errors coming from the absence of camera calibration certificate. This process is known as self-calibration adjustment. In this case the Brown's physical model (14 parameters) was used, which compensates for most of the linear and nonlinear forms of film and lens distortions (Aguilar et al., 2010b). However, it is necessary a high number and accurate ground

control points to cope with this bundle adjustment. In this case we counted on 45 ground control points measured by means of DGPS technology. Furthermore, 44 independent check points (ICPs), not employed during the triangulation adjustment, were used to check the process accuracy. In this way, the root mean square error (RMSE) was calculated over the ICPs yielding the following results: RMSEx = 17.6 cm; RMSYy = 17.1 cm; RMSEz = 33.3 cm. That is a very good result which assures a theoretically well-oriented DSM by using LPS stereo-matching. In fact, this final 1977 DSM may be considered as the best of all possible ones, but it also was very time-consuming and costly to obtain.
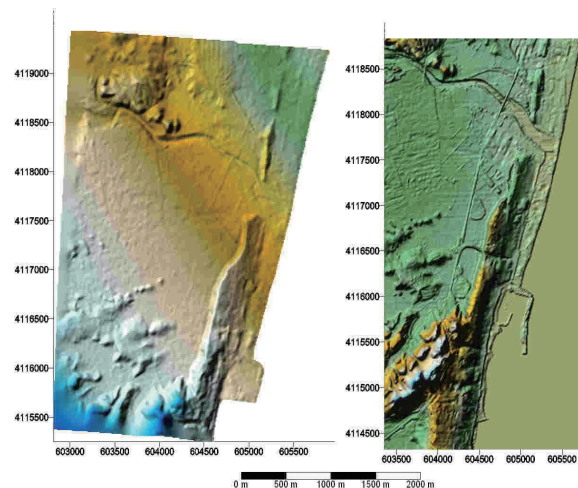

Figure 3. Photogrammetrically-derived CEMs corresponding to 1977 (left) and 2001 (right). Reference system UTM-ETRS89.

3.2.2. Data corresponding to 2001: The reference CEM corresponding to 2001 was a 10 m grid-spacing DTM produced by the Andalusia Regional Government (Spain) throughout a photogrammetric flight taken in 2001 at an approximated scale of 1:20000. This original DTM was transformed from UTM European Datum 1950 and orthometric heights to the new Spanish official geodetic system called the European Terrestrial Reference System (ETRS89) and elipsoidic heights above GRS80 ellipsoid. The corresponding DTM accuracy was estimated upon 62 DGPS check points located at open terrain, yielding a vertical RMSE value around 1.34 m. The historical CEM to geo-reference (1977) and the reference CEM (2001) are depicted in Figure 3 as 3D surface maps.

4. RESULTS AND DISCUSSION

4.1 Automatic Shaded-Relief Image Matching

It is important to point out that the matching results may be very variable depending on the solar position. In fact, automated GCP location in two images consists of two steps. The first one extracts spatial features from each image. Then, the features are paired by correspondence matching. The success of the process depends, in part, on the similarity of the features in the two images, which is clearly related to the solar position. This is the reason because the proposed methodology treats to iteratively search for an optimal solution changing both solar azimuth and solar elevation. In Fig. 4 and 5 are depicted the matching results coming from different solar positions. In the case of the 135° solar azimuth, only 26 conjugated points were successfully

matched out of 2139 and 1368 key points found in 1977 and 2001 shaded-relief images respectively. However, in the case of 270º solar azimuth, only 23 conjugated points were finally extracted out of 2772 and 1751 key points detected in 1977 and 2001 shaded-relief images. It is important to highlight that the most important is not only the number of pairs achieved but the homogeneous distribution of those points upon the working area. In the presented example, seems to be that the shaded-relief corresponding to 135º solar azimuth obtained a better distribution than 270º solar azimuth did, above all when we notice that the north area is only sustained by one pair of conjugated points in the second case.
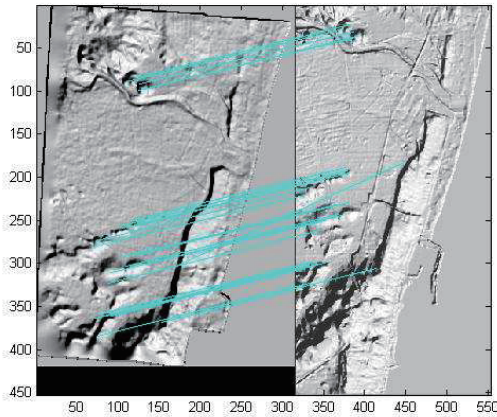

Figure 4. Results regarding automatic shaded-relief matching (image space) for a 135º solar azimuth and 45º solar elevation.
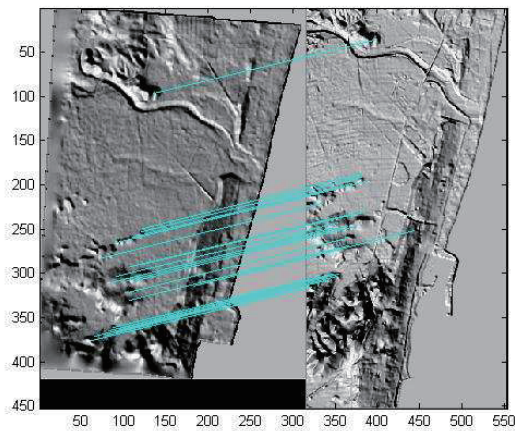

Figure 5. Results regarding automatic shaded-relief matching (image space) for a 270º solar azimuth and 45º solar elevation.

4.2 3D Helmert Adjustment

Table 1 shows the estimated transformation parameters for the computed 3D conformal transformation. It is important to highlight that, at a glance, the results regarding the two presented solar azimuths seem to be very similar. Even the accuracies obtained from the least squares variance-covariance matrix turned out to be slightly better in the case of 270º solar azimuth. But it only was a mathematical mirage, as we will check along the next section. In fact, though the residuals calculated at matched ground points were lower for the case of 270º azimuth than those coming from the case of 135º (Tables 2 and 3 respectively), the distribution around the whole working

area was quite better in the second case and, furthermore, more matched ground points were achieved. So we strongly recommend computing the 3D transformation with not less than 10 ground points, above all if the two matching CEMs correspond to a dynamic area where landscape change probability may be considered as very high.

Parameter	Estimated parameters			
	Solar azimuth 270º Solar elevation 45º		Solar azimuth 135º Solar elevation 45º	
	Value	Accuracy	Value	Accuracy
ΔX	-36.15 m	0.74 m	-38.81 m	0.99 m
ΔY	-8.35 m	0.77 m	-7.65 m	1.01 m
ΔZ	-10.97 m	0.74 m	-9.42 m	1.00 m
ΔΩ	0.0081º	0,00377º	0.0141º	0,00418º
ΔΦ	0.0174º	0,00172º	0.0162º	0,00372º
ΔK	-0.0116º	0,00489º	-0.0123º	0,00503º
λ	1.0006	0,00077	0.9954	0,00253

Table 1. Estimated values and accuracies for the computed seven parameters 3D Helmert adjustment (Geocentric coordinates with regard to GRS80 reference ellipsoid).

Matched GCPs	X (m)	Y (m)	Z (m)
1	-0.42	2.92	0.58
2	1.29	-3.30	-0.05
3	-0.79	1.99	0.52
4	-0.51	-2.78	0.04
5	-0.02	0.76	-0.79
6	0.46	0.40	-0.30

Table 2. Residuals in X, Y and Z after applying the 3D Helmert adjustment at the six utilized (out of 23) GCPs obtained by shaded-relief image matching (azimuth 270º, elevation 45º).

Matched GCPs	X (m)	Y (m)	Z (m)
1	1.09	2.46	-1.30
2	-2.55	2.68	3.02
3	2.21	-5.23	-2.07
4	0.30	2.36	-0.56
5	-1.04	3.41	0.77
6	1.73	1.32	-1.92
7	-3.53	3.72	4.26
8	1.82	-8.59	-2.47
9	-0.12	-1.64	0.38
10	0.08	-0.49	-0.11

Table 3. Residuals in X, Y and Z after applying the 3D Helmert adjustment at the ten utilized (out of 26) GCPs obtained by shaded-relief image matching (azimuth 135º, elevation 45º).

4.3 Surface Matching Results between 1977 and 2001

The wrong orientation of the preoriented CEM (course-oriented using ARO) can be observed in Figure 6. An accentuated rotation along a NW-SE axis is clearly visible,

leading to a disperse residuals histogram with an excessively high systematic vertical error (see Table 4).

Afterwards using the shaded-relief image algorithm, the initial CEM position has been notably corrected and the matching results have been clearly improved (Fig. 7). Because the algorithm checks different solar position previously selected by the user, it is possible to obtain different solutions and later checking which the best is. In this sense, the 135º solar azimuth would be preferred despite the slightly poorer results estimated during the adjustment process (Table 1). Indeed some signed statistical results are shown in Table 4. Notice that the standard deviation of the 135º solar azimuth case is quite near the RMSE estimated for the reference DTM (1.34 m). So the final matching may be considered as reasonably acceptable.
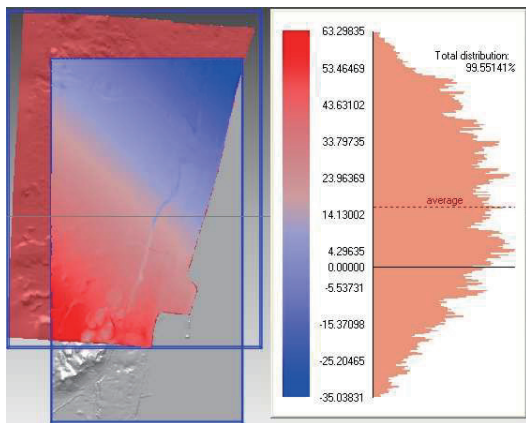

Figure 6. Map of signed vertical residuals (pre-oriented DSM 1977 – DTM 2001 within the overlap area) and corresponding histogram after applying the computed 3D Helmert parameters.
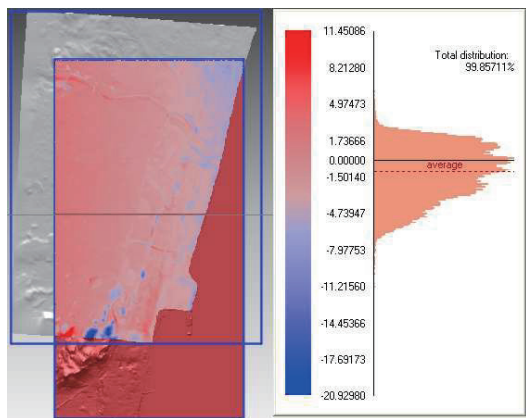

Figure 7. Map of signed vertical residuals (oriented DSM 1977 – DTM 2001 within the overlap area) and corresponding histogram after applying the computed 3D Helmert parameters. Case: 270º solar azimuth and 45º solar elevation shaded-relief.

Then, and judging numerical data and qualitative maps depicted in Table 4 and Figure 8, shaded-relief image matching could be use to coarsely co-register multi-temporal CEMs automatically without ground control points. It is needed to take into account that some of the gross errors detected in Figure 9 (green to red areas) may be actually no errors but landscape changes due to earthworks (cut and fills) projects. In this way the proposed methodology seems to be very robust because localized shaded-relief features used to compute the adjustment are usually

geomorphological features that remain relatively stable along time.

1977 DSM - 2001 DTM comparison	Signed residuals statistics			
	Mean (m)	Maximum (m)	Minimum (m)	Standard deviation (m)
Pre-oriented 1977 DSM – 2001 DTM	16.12	63.29	-35.03	22.15
1977 DSM (240º-45º) – 2001 DTM	-1.03	11.45	-20.92	2.70
1977 DSM (135º-45º) – 2001 DTM	-0.31	7.79	-15.18	1.89

Table 4. Signed residuals statistics for the overlap area corresponding to the comparison between 1977 shaded-relief oriented DSMs and 2001 reference DTM.
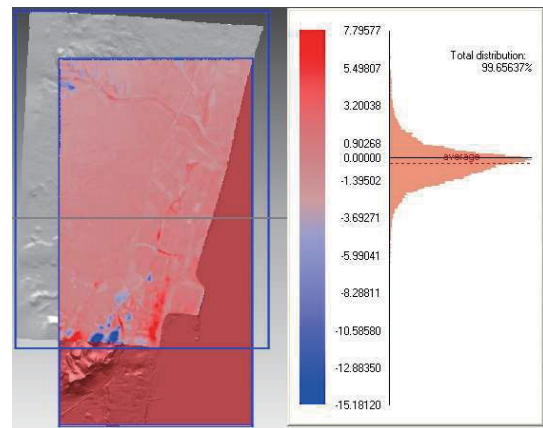

Figure 8. Map of signed vertical residuals (oriented DSM 1977 – DTM 2001 overlap area) and corresponding histogram after applying the computed 3D Helmert parameters. Case: 135º solar azimuth and 45º solar elevation shaded-relief.
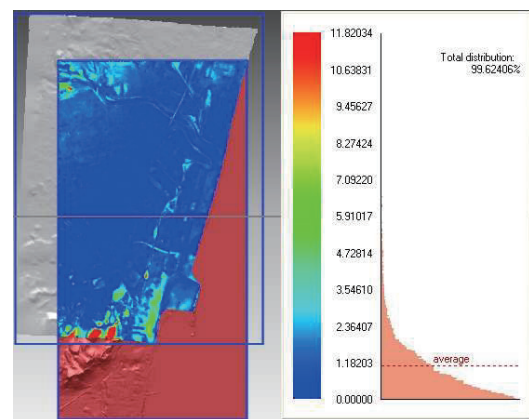

Figure 9. Map of absolute vertical residuals (oriented DSM 1977 – DTM 2001 overlap area). Case: 135º solar azimuth and 45º solar elevation shaded-relief.

The most important problem when registering multi-temporal DEMs is the intensity of temporal deformation or change occurred between the period of the study. In most surface matching algorithms the deformation area is restricted to not

much more than 50% by introducing the so-called differential model and improving the classic least Z-difference or LZD algorithm, but it is rather complex and needs a previous rough co-registration or knowing about the approximated transformation to carry out (Zhang and Cen, 2008). Our approach could be used as a first step headed up to later apply a LZD-based surface matching algorithm to refine the initial matching as much as possible. This second step should include weight functions based on M-estimators to make the computation more robust and resisting to the presence of outliers (Miller et al., 2008).

4.4 Comparison between the 1977 Photogrammetrically Oriented DSM and the Shaded-relief Matching Oriented DSM

As it was described in section 3.2.1, we previously made up "the best possible photogrammetric absolute orientation" for 1977 CEM by using a lot of GCPs and the self-calibration potential of LPS system to overcome the problem due to the absence of the camera calibration parameters. In Table 5 can be observed some residuals statistics from which it is possible to state that the performance of shaded-relief matching method may be considered as quite suitable. The fact is that the standard deviation is reasonably low, taking into account the flight scale and the corresponding CEM uncertainty (around 1.10 m). It is necessary to add that different stereo-matching methods to produce the 1977 CEM were utilised (that is ISAE Z/I and LPS systems). Hence there is an error from the get-go between both automatically generated CEMs that was estimated about 0.74 m (standard deviation) by means of a GCP-based surface matching approach.

DSM/DTM comparison	Maximum (m)	Minimum (m)	Standard deviation (m)
DSM (135°/45°) – PhotoDSM (1977)	6.40	-6.05	1.57
DSM (240°/45°) – PhotoDSM (1977)	5.28	-6.76	2.56
2001 DTM – 1977 PhotoDSM	8.34	-7.28	1.60

Table 5. Residuals statistics for the overlap area corresponding to the comparison between 1977 shaded-relief oriented DSMs and photogrammetrically oriented DSM (Photo DSM). It has been also added the comparison for 2001 DTM.

5. CONCLUSIONS

The results obtained from this work may be deemed as very promising, showing a good co-registration between reference and historical CEMs in heavily developed coastal areas. The point is the high efficiency and robustness demonstrated for historical CEM 3D geo-referencing when it was compared to costly and time-consuming traditional methods such as photogrammetric absolute orientation based on surveyed ground control points and self-calibrating bundle adjustment techniques. This preliminary approach could be used as a previous course matching to be subsequently refined by 3D robust surface matching.

6. ACKNOWLEDGEMENTS

7. REFERENCES

Aguilar, F.J., Carvajal, F., Aguilar, M.A., Agüera, F., 2007. Developing digital cartography in rural planning applications. *Computers and Electronics in Agriculture*, 55, pp. 89-106.

Aguilar, F.J., Mills, J.P., Delgado, J., Aguilar, M.A., Negreiros, J.G., Pérez, J.L., 2010a. Modelling vertical error in LiDAR-derived digital elevation models. *ISPRS Journal of Photogrammetry and Remote Sensing*, 65(1), pp. 103-110.

Aguilar, M.A., Aguilar, F.J., Negreiros, J.G., 2010b. Self-calibration methods for using historical aerial photographs with photogrammetric purposes. *Anales de Ingeniería Gráfica*, 21, pp. 33-40.

Andalusian Government, 2005. *Modelo digital del Terreno de Andalucía. Relieve y orografía*. Junta de Andalucía, Sevilla, Spain (on DVD).

Brock, J.C., Purkis, S.J., 2009. The emerging role of Lidar remote sensing in coastal research and resource management. *Journal of Coastal Research*, 53, pp. 1-5.

Cowell, P.J., Zeng, T.Q., 2003. Integrating uncertainty theories with GIS for modelling coastal hazards of climate change. *Marine Geodesy*, 26, pp. 5-18.

James, T.D., Murray, T., Barrand, N.E., Barr, S.L., 2006. Extracting photogrammetric ground control from LiDAR DEMs for change detection. *The Photogrammetric Record*, 21(116), pp. 312-328.

Lowe, D.G., 2004. Distinctive image features from scale-invariant keypoints. *International Journal of Computer Vision*, 60(2), pp. 91-110.

Miller, P., Mills, J.P., Edwards, S., Bryan, P., Marsh, S., Mitchell, H., Hobbs, P., 2008. A robust surface matching technique for coastal geohazard assessment and management. *ISPRS Journal of Photogrammetry and Remote Sensing*, 63(5), pp. 529-542.

Titus, J.G., Anderson, K.E., Cahoon, D.R., Gesch, D.B., Gill, S.K., Gutierrez, B.T., Thieler, E.R., Williams, S.J., 2009. Coastal sensitivity to sea-level rise; a focus on the mid-Atlantic region. U.S. Environmental Protection Agency, National Oceanic and Atmospheric Administration, U.S. Geological Survey. U.S. Climate Change Science Program synthesis and assessment product 4.1, 320 pp.

Webster, T.L., Forbes, D.L., Mackinnion, E., Roberts, D., 2006. Flood-risk mapping for storm-surge events and sea-level rise using LiDAR for southeast New Brunswick. *Canadian Journal of Remote Sensing*, 32(2), pp. 194-211.

Zhang, T., Cen, M., 2008. Robust DEM co-registration method for terrain changes assessment using least trimmed squares estimator. *Advances in Space Research*, 41, pp. 1827-1835.